

Detecting Pulp Stones with Automatic Deep Learning in Bitewing Radiographs: A Pilot Study of Artificial Intelligence

Ali Altındağ^{1,*}, Sultan Uzun², İbrahim Şevki Bayrakdar³ and Özer Çelik⁴

¹Assist. Prof., Department of Dentomaxillofacial Radiology, Necmettin Erbakan University, Faculty of Dentistry, Konya, Turkey and ²Res Assist., Department of Dentomaxillofacial Radiology, Necmettin Erbakan University, Faculty of Dentistry, Konya, Turkey and ³Assoc. Prof., Department of Dentomaxillofacial Radiology, Eskişehir Osmangazi University, Faculty of Dentistry, Eskişehir, Turkey and ⁴Dr., Department of Mathematics-Computer, Eskişehir, Eskişehir Osmangazi University, Faculty of Science, Turkey

*Corresponding Author; alialtindag1412@gmail.com

Abstract

Purpose: This study aims to examine the diagnostic performance of detecting pulp stones with a deep learning model on bite-wing radiographs.

Materials and Methods: 2203 radiographs were scanned retrospectively. 1745 pulp stones were marked on 1269 bite-wing radiographs with the CranioCatch labeling program (CranioCatch, Eskişehir, Turkey) in patients over 16 years old after the consensus of two experts of Maxillofacial Radiologists. This dataset was divided into 3 groups as training (n = 1017 (1396 labels), validation (n = 126 (174 labels)), and test (n = 126) (175 labels) sets, respectively. The confidence score of all tags was 84.04%; the trust of presence tags score of 85.82% and the confidence score of no labels were found to be 82.25%. The deep learning model was developed using Mask R-CNN architecture. A confusion matrix was used to evaluate the success of the model.

Results: The results of precision, sensitivity, and F1 obtained using the Mask R-CNN architecture in the test dataset were found to be 0.9115, 0.8879, and 0.8995, respectively.

Conclusions: Deep learning algorithms can detect pulp stones. With this, clinicians can use software systems based on artificial intelligence as a diagnostic support system. Mask R-CNN architecture can be used for pulp stone detection with approximately 90% sensitivity. The larger data sets increase the accuracy of deep learning systems. More studies are needed to increase the success rates of deep learning models.

Key words: artificial intelligence; bite-wing radiography; deep learning; pulp stone

Introduction

The pulp may show degenerative changes throughout life under the influence of many external or internal factors. As a result of factors exceeding the physiological tolerance limit, pathology mechanisms begin to operate in the pulp, and the morphological and histological structures of the pulp tissue deteriorate.¹ Pulp stones (PS), also called denticles or nodules, which can be detected in the primary and permanent dentition, are calcified structures observed in the dental pulp. Pulp stones can occur in the dental pulp, which is in good health, diseased, or even unerupted tooth.² Even though pulp calcifications have been linked to epithelial-pulp interactions, circulatory disorders in the pulp, degenerations, periodontal disease,

caries, orthodontic treatment, chronic inflammation, age, gender, genetic predisposition, and idiopathic, its exact cause is unknown.³ When looking at the factors related to the incidence of PS, the incidence of PS increases with age.⁴⁻⁶ There is no consensus about the affection of crown restorations, caries, or operated teeth. Although some studies have found that these factors increase the formation of PS,^{5,7-9} some have reported that they are not associated with crown status.¹⁰ PS are in the form of a more compact degenerative mass compared to dystrophic calcifications. PS does not have a distinct shape but is often found to be round or oval in shape. Despite its smooth contours generally, it can also rarely have irregular contours.¹¹ It may be large enough to cover the entire pulp chamber or small enough to be detected microscopically.³ Depending on

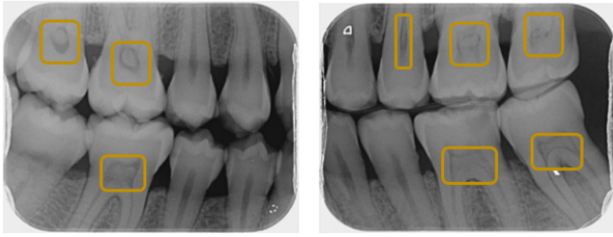


Figure 1. PS shown with a yellow frame on posterior teeth

their location, PS may be embedded in dentin, free, or adherent. It may be located more frequently in the coronal part of the pulp or less frequently in the radicular part (Figure 1). Free denticles are the most common stones on radiographs. The researchers stated that the classification according to the locations may need more accuracy. Due to the different cross-sectional angles, a genuinely cohesive stone can be seen.¹ PS can be detected histologically and radiologically.^{6,10,12,13} When histological and radiological evaluations are considered, the incidence of histologically observed PS is higher.^{6,13} In order to detect calcification radiologically, a certain mineralization level reaches a certain size of ($>200\mu\text{m}$).^{3,14} The radiographic boundaries of calcifications are often extremely difficult to determine, even if there is sufficient mineralization and size. However, radiographs are the only non-invasive and clinically detectable calcification method.¹⁴ Depending on the used radiographic technique, study type, and design, the prevalence of PS varies from %8-9.¹⁵ Inadvertently, wrong or inadequate diagnosis may occur in busy clinics or because of inexperienced dentists, such as pulp stones. Computer-aided systems have been improved in dental imaging to reduce misdiagnosis and assist doctors.¹⁶ Artificial intelligence (AI), which is very popular and increasingly used in dentistry such as the studies on caries detection, periodontal and apical lesions, tooth numbering, and oral pathologies, is a term that includes the machines' ability to mimic human knowledge and behavior. Machine learning (ML) and deep learning (DL) are applications of algorithms that analyze data and initiate models that identify certain properties of that data, allowing future predictions on new datasets.¹⁷ Computers are not explicitly programmed in machine learning, artificial intelligence's sub-branch. Despite this, it can perform its tasks by analyzing existing data relationships. Deep learning (DL), one of the sub-branch of machine learning (ML), is a working area that covers artificial neural networks and similar ML algorithms with one or more hidden layers (Figure 2).¹⁸ With the quick development in deep learning, convolutional neural networks (CNN), and artificial neural networks, are used in object detection and processing. They are the basic building blocks of image segmentation. The object detection method is suitable for many applications such as classification,^{19,20} and human face recognition.²¹ Zone recommendation-based object detection algorithms are mainly R-CNN,²² SPP-net,²³ Fast R-CNN,²⁴ Faster R-CNN,²⁵ R-FCN,²⁶ FPN,²⁷ and Contains Mask-RCNN. The purpose of this study is to evaluate the diagnostic DL model (Mask R-CNN) designed to detect PS on bite-wing radiography.

Material and Methods

This study was carried out with the dataset created from the classification of images obtained from patients who came to Necmettin Erbakan University, Faculty of Dentistry Maxillofacial Radiology Clinic, between January 2020 and September 2021. Necmettin Erbakan University Faculty of Dentistry Pharmaceutical and Non-Device Research Ethics Committee approved the study protocol (Approval Date and Number 30.06.2022, 2022/154). It was conducted in line with the Helsinki Declaration of Human Rights guidelines. Bite-wing radiographs of 2203 patients with an age range of over

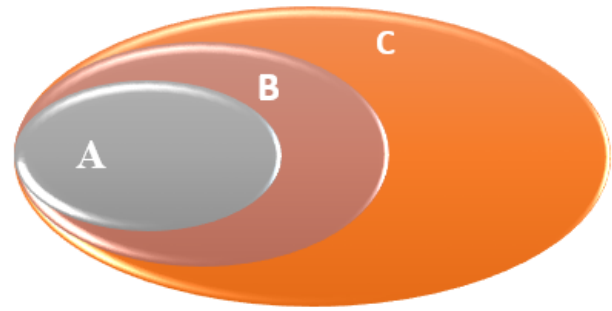


Figure 2. The relationship of deep learning method with other AI techniques (AI (C) , ML (B) , DL (A))

16 years were evaluated, retrospectively. Exclusion Criteria;

- Patients under 16 years of age
- Radiographs with poor quality or artifacts
- Bite-wing images of individuals with any dental disease (Dentinogenesis Imperfecta, Dentin dysplasia, etc.)
- Bite-wing images of individuals who have undergone resection and cancer surgery in the maxillofacial region

Inclusion Criteria;

- Over 16 years old patients
- Maxillary and mandibular posterior teeth except for third molars
- Radiographs of patients without extensive bone and dental pathology
- Patients with diagnostically acceptable bite-wing radiographs

Two examiners observed the radiographs. Reliability was obtained as a result of repeated measurements. Each observer re-evaluated 100 randomly selected radiographs after 3 weeks, and intra-observer agreement values were calculated. For inter-observer agreement, 200 images were reexamined by two radiologists. Marking was done in the presence of definite PS, the boundaries of which could be drawn. Detection of PS occurred after consensus, and interobserver agreement was observed at a rate of 0.917. After the consensus of two experts Maxillofacial Radiologists, PS was labeled with the polygonal type labeling method with the CranioCatch labeling program (CranioCatch, Eskisehir, Turkey). In the present study, the Mask R-CNN architecture, a DL-based image segmentation model, was used. Mask R-CNN, is an extension of Faster R-CNN and works by adding a branch to predict an object mask (Region of Interest) in parallel to the existing branch for bounding box recognition. The Mask R-CNN's core element is pixel-to-pixel alignment. This is the main missing piece of Fast/Faster R-CNN. Mask R-CNN is easy to implement and train.²⁸ Model success was evaluated with the confusion matrix. The confusion matrix is a metric that visualizes system prediction and real situations and reads results to evaluate the performance of machine learning algorithms.²⁹

This dataset was divided into three groups;

- Training group (n = 1017 (1396 labels))
- Validation group (n = 126 (174 labels))
- Test group (n = 126 (175 labels)) sets.

The proposed artificial intelligence (AI) model (CranioCatch, Eskisehir, Turkey) approach for PS detection is based on a deep CNN using 200,000 epochs trained with Mask R-CNN inception v2 (COCO) with a 0.0002 learning rate. PS must be specified using a separate deep CNN. The training was performed using 7000 steps on a PC with 16GB RAM and the NVIDIA GeForce GTX 1660 TI. The training and validation datasets were used to predict and generate

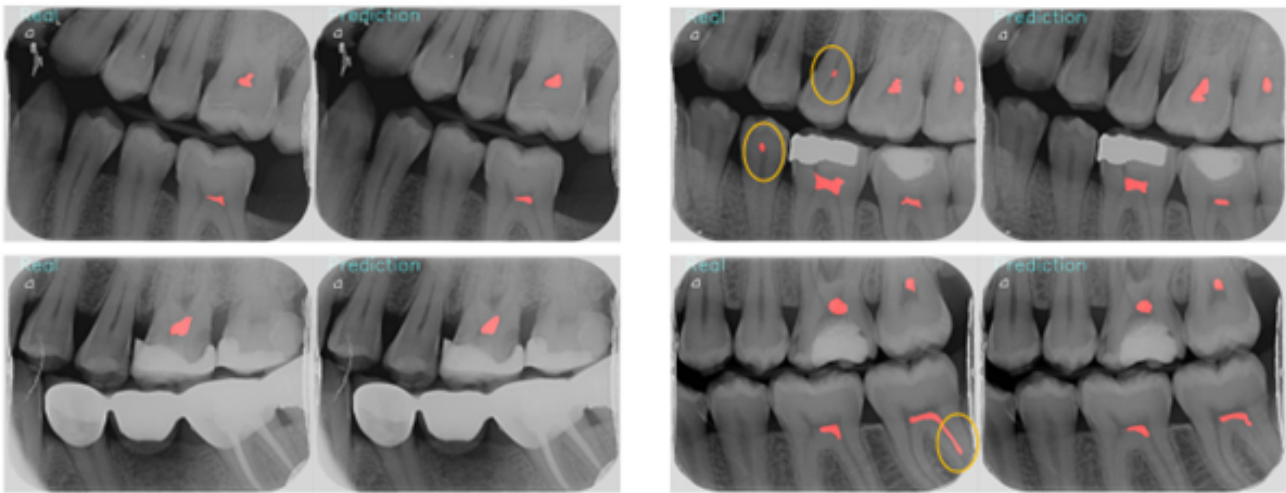


Figure 3. A few examples of comparative evaluation of expert markings and artificial intelligence markings

Table 1. F1, sensitivity and precision results of artificial intelligence model obtained using Mask R-CNN architecture

Results					
True Positive (TP)	False Positive (FP)	False Negative (FN)	Sensitivity	Precision	F1 score
103	10	13	0,8879	0,9115	0,8995

optimal CNN algorithm weight factors. The success of the model was evaluated with the confusion matrix. The data in this matrix is often used to evaluate the performance of systems, being a meaningful table that summarizes predicted and actual situations. The metrics used for model success are as follows:

- True positive (TP): PS marked by experts and AI
- False negative (FN): PS labeled by experts but not labeled by AI
- False positive (FP): PS not labeled by experts but labeled by AI

After the calculation of TP, FN, and FP; the following metrics were calculated: Sensitivity (recall): $TP/(TP+FN)$; Precision: $TP/(TP+FP)$; F1 score: $2TP/(2TP+FP+FN)$.

Results

Kappa values for intra-observer and inter-observer agreement were found to be 0.982 (Observer 1), 0.988 (Observer 2), and 0.917, respectively. The bite-wing radiographs of 1269 patients had pulp chamber calcifications. When the radiographs in which the algorithm was incomplete or faulty were examined, it was observed that the Mask R-CNN architecture was insufficient to detect pulp stones in the mandible and root pulp due to superpositions and artifacts. Since the root pulp is also less visible on bite-wing radiographs than the coronal pulp, the smallness of the dataset in the root pulp played a role in the incomplete or erroneous detection (Figure 3). Respectively, the results of precision, sensitivity, and F1 obtained using the Mask R-CNN architecture in the test dataset were found to be 0.9115, 0.8879, and 0.8995 (Table 1).

Discussion

The studies on PS are mostly histological and there are also few radiological studies.^{6,10,12,13} Willman et al. evaluated calcifications with histological and radiological analyzes comparatively. The incidence of PS was found to be higher histologically. The factors which affect this result are the small size of the PS in the initial stage, the necessity of its diameter to be more than 200 μ m for radiological evaluation, and the superpositions that occur in the

radiographs. However, the disadvantages of histological studies should not be ignored. Histological studies are only useful as an ex vivo method and focus on a specific part of the pulp, not the whole pulp. As a result of the limited evaluated parts from the teeth, there will be calcified structures that are overlooked.^{6,9,13} The fact that radiological evaluation is non-invasive and its routine use during dental examination makes radiological evaluation advantageous. Several existing studies have used different radiographs to diagnose pulp stones. Tamse et al.¹⁰ examined both bite-wing and periapical radiographs to identify pulp stones and to check the differences between these two radiographic techniques. In the study, only 14 of the evaluated 1380 teeth were found different, so between the two techniques, no statistically significant difference was observed. Turkal et al.³⁰ demonstrate that due to the inability of panoramic radiographs in giving a clear image of the posterior teeth, bite-wing radiographs show superiority. On the other hand, their study showed that bite-wing radiographs could not evaluate all jaw teeth simultaneously. Taysoker et al.³¹ detected 15.9% (252 of 1.616) more PS than CBCT in digital panoramic radiography (DPR). DPR, may over/under estimate the prevalence of PS due to image distortion and superimposition. Although CBCT is the best imaging model for the detection of PS as it prevents superpositions and has greater specificity, the radiation dose is too high for routine radiographic examination.³² Taking into account previous studies, bite-wing radiographs were used to detect the presence of pulp stones in this study. Artificial intelligence in medicine has accelerated with the improvement of DL and neural methods. It has been used to solve problems in many clinical areas. With the increase in artificial intelligence applications in medicine, its use has started to increase in dentistry.³³ Artificial intelligence's potential accuracy have evaluated in various studies by interpreting medical images (magnetic resonance imaging, X-rays, computed tomography, positron emission tomography), and the results are promising.³⁴ Artificial intelligence using ML and/or DL in dental practice shows excellent promise for various application areas. Although it requires extensive research to determine the robustness of AI models, AI is expected to become part of the dentist's examination kit soon. However, it needs more discussion on the ethical aspects of AI.¹⁷ ML and DL are computational systems that learn over time based on experience. While ML is sufficient for the classification of simple

numerical data; DL is used for analyzing wide imaging sets and complex data. DL applications are therefore becoming increasingly important in dental practice, particularly in radiology.¹⁷ The aim of AI studies in dental radiology is to make evaluations of routine, simple, and frequently encountered radiographs, saving time for more complex cases, and also helping inexperienced dentists to diagnose. Image segmentation, pixel-level classification, is the task of bringing together parts of an image that belong to the same object class. Image segmentation is widely applied in medical applications such as determining tumor boundaries or measuring tissue volumes. Image segmentation models based on deep learning often achieve the best accuracy rates in popular benchmarks, resulting in a paradigm shift in the field.³⁵ The R-CNN architecture was designed to solve region-based image detection tasks. R-CNN architecture, which was improved into Faster R-CNN, forms the basis of Mask R-CNN. Mask R-CNN, is state-of-the-art in terms of image segmentation and instance segmentation.²⁸ He et al.²⁸ evaluated object recognition methods comparatively, object detection single model results (bounding box AP) were compared with the latest technology in test development. Masking R-CNN using ResNet-101-FPN outperformed key variants of all previous state-of-the-art models (mask output was ignored in these experiments). The gains of Mask R-CNN come from using RoIAlign (+1.1 APbb), multitasking training (+0.9 APbb), and ResNeXt-101 (+1.6 APbb). The superiority of Mask R-CNN over other image segmentation methods are the pixel-to-pixel alignment, fast experimentation with enabling a fast system and ensuring round shape pixels. Round pixels can be useful in detecting pulp stones, which are generally oval in contour, by DL methods. In the past object detection studies based on the deep learning algorithm, Bayraktar et al.,³⁶ used YOLO architecture to diagnose dental caries in digital bite-wing radiographs. The result of the accuracy, sensitivity, and specificity was 80%, 75%, and 83, respectively. Rashid et al.,³⁷ studied on localize dental cavities from real-time mixed photographic images with Mask R-CNN architecture. The correctness of datasets was found up to 96%, and the accuracy of the proposed system was between 78% and 92%. The precision/accuracy (P) rates in colored photographs were 88.02, in X-ray/ grayscale radiographs was 95.75, and in mixed was 81.02. Also, Kumar et al.³⁸ (SVM model, P: 86.70), Koutsouri et al.³⁹ (Inception CNN architecture, P: 82.00), and Vashishth et al.⁴⁰ (U-Net architecture, P:80) used X-Ray/Grayscale radiographs to diagnose dental cavities. In comparison with all these studies, Mask R-CNN architecture with the P:95.75 shows the highest result to diagnose. Mask R-CNN architecture is used in many areas such as caries detection and tooth numbering/segmentation in dentistry. Mouselos et al.,⁴¹ detected occlusal caries on 88 intraoral radiographs according to ICDAS scoring using Mask R-CNN architecture, recall, precision, and F-score values were 0.889, 0.778, and 0.667, respectively. Silva et al.,⁴² studied thoroughly the literature on segmentation methods applied in dental imaging. MASK R-CNN achieved average results of 92% (accuracy), 96% (specificity), 84% (precision), 76% (recall), and 79% (F-score), in this study. These values indicate that MASK R-CNN achieved a low number of false positives and false negatives. Although it is not possible to directly compare these results with the other unsupervised methods, one can be assured that no other unsupervised method achieved more than 70% in all the metrics at once. In the literature review, there is any study except the conference statement of Selmi et al., pulp stones are detected by using artificial intelligence-based software.⁴³ Convolutional Neural Network (CNN) was used. 76.4% with a Medium Gaussian Support Vector Machine (SVM) of Residual Network 50 (ResNet-50). They concluded that Inception v3 achieved a correct prediction rate of 73.1% with the identical classifier. ResNet-50 also has a 7% lower false positive rate than Inception v3s, giving it the potential to experiment more. In the present study, Mask R-CNN architecture, with about %90 sensitivity, can diagnose PS. The results show that Mask R-CNN architecture is better than the other object detection algorithms to diagnose PS. In AI studies, the homoge-

neous and balanced separation of training and test sets as possible is an important issue that increases working performance.⁴⁴ In our study, the labeled PS (1269) was higher than the labeled without PS (934). It caused the system to train more with the label "with PS". Even though, the sensitivity is high in the present study, a balanced training model can result in higher precision. On the other hand, the training model was used to look for the pulp chambers in the right place and did not identify another area in the pulp chamber radiodensity on the bite-wing as the pulp chamber.

Conclusion

Deep learning algorithms can detect pulp stones; with this, software systems supported by artificial intelligence can be used to assist dentists in the examination. Mask R-CNN architecture can be used for pulp stone detection with approximately 90% sensitivity. The accuracy rates in deep learning techniques increase as the dataset grows. Evaluating more radiographs in training models makes better rates of success, so more data is needed for future studies.

Acknowledgements

This paper will be presented as an oral presentation at the 4th International Society of Oral and Maxillofacial Radiology Congress on 19-23rd of October, in Izmir, Turkey. This project has not received any financial support.

Author Contributions

A.A. and S.U. scanned and marked pulp stones on bitewing radiographs. I.S.B. and O.C. resized all images, created and evaluated the model. All authors contributed to the preparation of the full text.

Conflict of Interest

Authors declare that they have no conflict of interest.

Authors' ORCID(s)

A.A. [0000-0001-8549-5193](https://orcid.org/0000-0001-8549-5193)
 S.U. [0000-0003-3743-055X](https://orcid.org/0000-0003-3743-055X)
 I.S.B. [0000-0001-5036-9867](https://orcid.org/0000-0001-5036-9867)
 O.C. [0000-0002-4409-3101](https://orcid.org/0000-0002-4409-3101)

References

1. Mete U. Diş Pulpasında Meydana Gelen Kalsifikasyonlar. J Istanbul Univ Fac Dent. 2013;13(2):167-188. doi:<https://dergipark.org.tr/tr/pub/jiufd/issue/8944/111477>.
2. Langeland K, Rodrigues H, Dowden W. Periodontal disease, bacteria, and pulpal histopathology. Oral Surg Oral Med Oral Pathol. 1974;37(2):257-270. doi:[10.1016/0030-4220\(74\)90421-6](https://doi.org/10.1016/0030-4220(74)90421-6).
3. Goga R, Chandler NP, Oginni AO. Pulp stones: a review. Int Endod J. 2008;41(6):457-468. doi:[10.1111/j.1365-2591.2008.01374.x](https://doi.org/10.1111/j.1365-2591.2008.01374.x).
4. Hill TJ. Pathology of the dental pulp. J Am Dent Assoc. 1934;21(5):820-844.
5. Sayegh F, Reed A. Calcification in the dental pulp. Oral Surg Oral Med Oral Pathol. 1968;25(6):873-882. doi:[10.1016/0030-4220\(68\)90165-5](https://doi.org/10.1016/0030-4220(68)90165-5).
6. Willman W. Numerical incidence of calcification in human pulps. J Dent Res. 1932;14:660. doi:[10.11471/shikahozon.50.752](https://doi.org/10.11471/shikahozon.50.752).

7. James V. Early pulpal calcifications of permanent teeth of young individuals. *J Dent Res*. 1958;37:973.
8. James VE, Schour I, Spence JM. Biology of the pulp and its defense. *J Am Dent Assoc*. 1959;59(5):903–911. doi:10.14219/jada.archive.1959.0247.
9. Sundell JR, Stanley HR, White CL. The relationship of coronal pulp stone formation to experimental operative procedures. *Oral Surg Oral Med Oral Pathol*. 1968;25(4):579–589. doi:10.1016/0030-4220(68)90303-4.
10. Tamse A, Kaffe I, Littner M, Shani R. Statistical evaluation of radiologic survey of pulp stones. *J Endod*. 1982;8(10):455–458. doi:10.1016/S0099-2399(82)80150-7.
11. Deva V, Mogoantă L, Manolea H, Pancă OA, Vătu M, Vătăman M. Radiological and microscopic aspects of the denticles. *Rom J Morphol Embryol*. 2006;47(3):263–268.
12. Moss-Salentijn L, Klyvert MH. Epithelially induced denticles in the pulps of recently erupted, noncarious human premolars. *J Endod*. 1983;9(12):554–560. doi:10.1016/S0099-2399(83)80060-0.
13. Willman W. Calcifications in the pulp. *Bur*. 1934;34:73–76.
14. Nayak M, Kumar J, Prasad LK. A radiographic correlation between systemic disorders and pulp stones. *Indian J Dent Res*. 2010;21(3):369. doi:10.4103/0970-9290.70806.
15. Moss-Salentijn L, Hendricks-Klyvert M. Calcified structures in human dental pulps. *J Endod*. 1988;14(4):184–189. doi:10.1016/S0099-2399(88)80262-0.
16. Hung K, Montalva C, Tanaka R, Kawai T, Bornstein MM. The use and performance of artificial intelligence applications in dental and maxillofacial radiology: A systematic review. *Dentomaxillofac Radiol*. 2020;49(1):20190107. doi:10.1259/dmfr.20190107.
17. Pauwels R. A brief introduction to concepts and applications of artificial intelligence in dental imaging. *Oral Radiol*. 2021;37(1):153–160. doi:10.1007/s11282-020-00468-5.
18. Kaur P, Singh G, Kaur P. A review of denoising medical images using machine learning approaches. *Curr Med Imaging*. 2018;14(5):675–685. doi:10.2174/1573405613666170428154156.
19. Jia Y, Shelhamer E, Donahue J, Karayev S, Long J, Girshick R, et al. Caffe: Convolutional architecture for fast feature embedding. In: *Proceedings of the 22nd ACM international conference on Multimedia*; 2014. p. 675–678. doi:10.1145/2647868.2654889.
20. Krizhevsky A, Sutskever I, Hinton GE. Imagenet classification with deep convolutional neural networks. *Commun ACM*. 2017;60(6):84–90. doi:10.1145/3065386.
21. Yang Z, Nevatia R. A multi-scale cascade fully convolutional network face detector. In: *2016 23rd International Conference on Pattern Recognition (ICPR)*. IEEE; 2016. p. 633–638. doi:10.1109/ICPR.2016.7899705.
22. Girshick R, Donahue J, Darrell T, Malik J. Rich feature hierarchies for accurate object detection and semantic segmentation. In: *Proceedings of the IEEE conference on computer vision and pattern recognition*; 2015. p. 580–587. doi:10.1109/CVPR.2014.81.
23. He K, Zhang X, Ren S, Sun J. Spatial pyramid pooling in deep convolutional networks for visual recognition. *ECCV*. 2015;37(9):1904–1916. doi:10.1109/TPAMI.2015.2389824.
24. Girshick R. Fast r-cnn. In: *Proceedings of the IEEE international conference on computer vision*; 2015. p. 1440–1448.
25. Ren S, He K, Girshick R, Sun J. Faster r-cnn: Towards real-time object detection with region proposal networks. *Advances in neural information processing systems*. 2015;28.
26. Dai J, Li Y, He K, Sun J. R-fcn: Object detection via region-based fully convolutional networks. *Adv Neural Inf Process Syst*. 2016;29. doi:10.48550/arXiv.1605.06409.
27. Lin TY, DollAr P, Girshick R, He K, Hariharan B, Belongie S. Focal loss for dense object detection. In: *Proceedings of the IEEE conference on computer vision and pattern recognition*; 2011. p. 2980–2988.
28. He K, Gkioxari G, DollAr P, Girshick R. Mask r-cnn. In: *Proceedings of the IEEE international conference on computer vision*; 2017. p. 2961–2969. doi:10.1109/ICCV.2017.322.
29. Santra A, Christy CJ. Genetic algorithm and confusion matrix for document clustering. *Int J Comput Sci Issues*. 2012;9(1):322–328.
30. Turkal M, Tan E, Uzgur R, Hamidi M, Colak H, Uzgur Z. Incidence and distribution of pulp stones found in radiographic dental examination of adult Turkish dental patients. *Ann Med Health Sci Res*. 2013;3(4):572–576. doi:10.4103/2141-9248.122115.
31. Tassoker M, Magat G, Sener S. A comparative study of cone-beam computed tomography and digital panoramic radiography for detecting pulp stones. *Imaging Sci Dent*. 2018;48(3):201. doi:10.5624/isd.2018.48.3.201.
32. Hsieh CY, Wu YC, Su CC, Chung MP, Huang RY, Ting PY, et al. The prevalence and distribution of radiopaque, calcified pulp stones: A cone-beam computed tomography study in a northern Taiwanese population. *J Dent Sci*. 2018;13(2):138–144. doi:10.1016/j.jds.2017.06.005.
33. Orhan K, Bayraktar I, Ezhov M, Kravtsov A, Özyürek T. Evaluation of artificial intelligence for detecting periapical pathology on cone-beam computed tomography scans. *Int Endod J*. 2020;53(5):680–689. doi:10.1111/iej.13265.
34. El-Damanhoury HM, Fakhruddin KS, Awad MA. Effectiveness of teaching International Caries Detection and Assessment System II and its e-learning program to freshman dental students on occlusal caries detection. *Eur J Dent*. 2014;8(04):493–497. doi:10.4103/1305-7456.143631.
35. Minaee S, Boykov YY, Porikli F, Plaza AJ, Kehtarnavaz N, Terzopoulos D. ECCV. *IEEE Transactions on Pattern Analysis and Machine Intelligence*. 2021;35:23–3542. doi:10.1109/TPAMI.2021.3059968.
36. Bayraktar Y, Ayan E. Diagnosis of interproximal caries lesions with deep convolutional neural network in digital bitewing radiographs. *Clin Oral Investig*. 2022;26(1):623–632. doi:10.1007/s00784-021-04040-1.
37. Rashid U, Javid A, Khan AR, Liu L, Ahmed A, Khalid O, et al. A hybrid mask RCNN-based tool to localize dental cavities from real-time mixed photographic images. *PeerJ Comput Sci*. 2022;8:e888. doi:10.7717/peerj-cs.888.
38. Kumar A, Bhaduria HS, Singh A. Descriptive analysis of dental X-ray images using various practical methods: a review. *PeerJ Comput Sci*. 2021;7:e620. doi:10.7717/peerj-cs.620.
39. Koutsouri GD, Berdouses E, Tripoliti EE, Oulis C, Fotiadis DI. Detection of occlusal caries based on digital image processing. In: *13th IEEE International Conference on BioInformatics and Bio-Engineering*. IEEE; 2013. p. 1–4. doi:10.1109/BIBE.2013.6701708.
40. Vashishth A, Kaushal B, Srivastava A. Caries detection technique for radiographic and intra oral camera images. *Int J Soft Comput Eng*. 2014;4(2):2231–2307.
41. Moutselos K, Berdouses E, Oulis C, Maglogiannis I. Recognizing occlusal caries in dental intraoral images using deep learning. In: *2019 41st Annual International Conference of the IEEE Engineering in Medicine and Biology Society (EMBC)*. IEEE; 2019. p. 1617–1620. doi:10.1109/EMBC.2019.8856553.
42. Silva G, Oliveira L, Pithon M. Automatic segmenting teeth in X-ray images: Trends, a novel data set, benchmarking and future perspectives. *Expert Syst Appl*. 2018;107:15–31. doi:10.1016/j.eswa.2018.04.001.
43. Selmi A, Syed L, Abdulkareem B. Pulp Stone Detection Using Deep Learning Techniques. In: *EAI International Conference on IoT Technologies for HealthCare*. Springer; 2021. p. 113–124. doi:10.1007/978-3-030-99197-5_10.
44. Koçoğlu F, Özcan T. Dengeli-dengesiz veri seti dagiliminin asiri ogrenme makinesi yonetimi performansina etkisi; 2018. .